A&A manuscript no.
(will be inserted by hand later)

Your thesaurus codes are:
07 (11.01.2; 11.19.1; 11.14.1; 13.25.2; 02.12.3;)

ASTRONOMY
AND
ASTROPHYSICS
3.3.1997

The nature of the FHIL winds from AGN ⋆

U. Erkens, I. Appenzeller, and S. Wagner

Landessternwarte Königstuhl, D-69117 Heidelberg, Federal Republic of Germany

Received date; accepted date

Abstract. In order to investigate the properties of the forbidden high-ionization lines (FHILs) in the spectra of AGN we observed 15 Seyfert galaxies and two emission line radio galaxies with a spectral resolution of about 2000 in the spectral range 3200 - 11 000 Å. All observed spectra contained significant [Ne V] and [Fe VII] lines. The spectra of the Seyfert nuclei (but not the radio galaxies) showed also [Fe X], [Fe XI], and in some cases [Fe XIV] emission. Our data confirm that the FHILs are on average broader and blueshifted relative to the lines of lower ionization stages. The amount of the blueshift was found to be correlated with the line widths. Large blueshifts were observed only for lines with high FWHM. An analysis of the line ratios indicates for the FHIL producing plasma an average electron temperature of about 7×10^4 K. Comparing our results with ROSAT data we found a correlation between the X-ray spectral index and the strength of the FHILs. Strong FHIL emission was found to occur predominantly in objects with a soft X-ray excess. We propose that the FHIL emission and the X-ray absorption edges in AGN ("warm absorbers") are related and that both phenomena result from a radiation driven warm wind originating in the central region of the AGN.[1]

Key words: Galaxies: active – Galaxies: Seyfert – Galaxies: nuclei – X-rays: galaxies – Line: profiles

1. Introduction

Spectroscopic observations carried out by different authors during the past two decades established the presence of emission lines with widths intermediate between those typical for the broad-line regions (BLR) and the narrow-line regions (NLR) in the spectra of AGN. In addition to weak broad wings of the strong [O III] lines of some AGN (cf. e.g. van Groningen and de Bruyn 1989) profiles or profile components of intermediate width are observed in particular at the forbidden lines of the higher ionization stages of Fe, Ne, and Si. In addition to being broader, these "coronal lines" or "forbidden high-ionization lines" (FHILs) are normally blueshifted relative to the low-ionization forbidden lines (cf. e.g. Grandi 1978, Wilson 1979, Osterbrock 1981, Pelat et al. 1981, Heckman et al. 1981, Atwood et al. 1982, De Robertis and Osterbrock 1984, 1986, Penston et al. 1984, Filippenko and Halpern 1984, Whittle 1985, Appenzeller and Östreicher 1988, Wilson and Nath 1990, Appenzeller and Wagner 1991, Giannuzzo et al. 1995, Thompson 1996, Wagner 1997) indicating an outflow of the gas emitting these features. At least in those cases where the FHILs are much broader than the narrow emission lines it is obvious that this emission cannot originate from the normal NLR gas (although the NLR - and even the ENLR - may well contribute to the cores and narrow components of the FHILs). On the other hand, since the FHILs are on average less broad than the BLR lines of Seyfert 1 galaxies and since intermediate width FHILs are also observed in Seyfert 2s, the FHIL emitting region cannot coincide with the BLR.

The absence of the intermediate width components in the profiles of emission lines from lower ionization stages and the observed line ratios (cf. e.g. Ward and Morris 1984) indicate for the FHIL emitting plasma a temperature which is significantly higher than that of the NLR and BLR gas. Since the temperature dependence of the cooling functions make it difficult to maintain a plasma in the required temperature range (of the order 10^5 K) the presence of the FHIL emitting gas provides particularly critical constraints on theoretical models of the AGN. Any selfconsistent model has to explain the presence and properties of these lines. Unfortunately, the FHIL lines observable in the visual and UV spectral range are relatively weak. Most data on these lines in the literature are, therefore, of limited accuracy, and not much is known about the systematic properties of these lines. In order to increase our knowledge of these spectral features we observed a sample of 15 Seyfert galaxies and 2 emission line radio galaxies to study the FHIL properties. 12 of the observed 15 Seyfert galaxies have been classified in the literature as Sey 1, two as Sey 2, and one as Sey 1.5. One of the Sey 1 objects (Mrk 1239) and the only Sey 1.5 in our program (Mrk

Send offprint requests to: I. Appenzeller

⋆ Based on observations collected at the German-Spanish Astronomical Centre, Calar Alto, operated by the Max-Planck-Institut für Astronomie, Heidelberg, jointly with the Spanish National Commission for Astronomy

[1] Tables A1 to A18 are only available in electronic form at the CDS (Strasbourg) via anonymous ftp to cdsarc.u-strasbg.fr (130.79.128.5) or via http://cdsweb.u-strasbg.fr/Abstract.html.

Table 1. The observed AGN and some basic FHIL parameters of these objects

Object	Type	z	E(B-V)	[Fe VII]/[OIII]		[Fe X]/[O III]		[Fe XI]/[O III]		[Fe VIII]/Hα	[Fe XI]/Hα
				Flux	FWHM	Flux	FWHM	Flux	FWHM	FWHM	FWHM
Mrk 975	Sey 1	.0491	0.04	0.094	1.54	?	br.	?	br.	0.44	?
Mrk 359	Sey 1.5	.0169	0.13	0.083	1.37	0.057	1.33	0.035	1.99	0.90	1.30
Mrk 573	Sey 2	.0171	0.20	0.010	1.03	0.004	1.15	0.002	1.25	0.93	1.14
NGC 1320	Sey 2	.0089	0.33	0.040	1.21	0.023	1.41	0.016	?	1.00	?
Akn 120	Sey 1	.0330	0.33	0.218	1.90	0.154	1.74	0.096	2.10	0.17	0.18
Mrk 9	Sey 1	.0390	0.33	0.142	2.40	0.071	2.26	0.055	2.62	0.36	0.39
Mrk 704	Sey 1	.0291	0.28	0.134	0.86	0.070	1.10	0.035	1.07	0.19	0.24
Mrk 705	Sey 1	.0285	0.10	0.090	1.07	0.052	1.04	0.020	?	0.28	?
Mrk 1239	Sey 1	.0194	0.17	0.110	1.66	0.083	1.83	0.072	2.30	1.03	1.43
NGC 4051	Sey 1	.0020	0.37	0.056	1.17	0.058	1.42	0.038	1.29	0.49	0.54
NGC 4395	Sey 1	.0010	0.20	0.006	2.77	0.002	2.39	0.000	?	2.05	?
Mrk 486	Sey 1	.0389	0.26	0.134	2.81	0.134	br.	?	br.	0.76	?
Mrk 871	Sey 1	.0340	0.14	0.049	?	0.044	?	?	?	?	?
Mrk 699	Sey 1	.0337	0.18	0.068	1.10	0.037	1.08	0.038	1.47	0.62	0.83
3C 390.3	RG	.0561	0.28	0.033	1.70	-	-	-	-	0.11	-
3C 445	RG	.0562	0.49	0.033	1.86	-	-	-	-	0.27	-
Akn 564	Sey 1	.0247	0.09	0.041	1.57	0.079	2.15	0.093	2.62	0.67	1.12
Mean:				0.079	1.63	0.062	1.58	0.042	1.86	0.64	0.80

359) have also been listed as Narrow-line Seyfert 1 galaxies by Osterbrock and Pogge (1985). Apart from the visual magnitude (≤ 15.5) the main selection criterium for our program objects was that the presence of FHILs had been reported before in the literature. However, in most cases these earlier results were based on spectra of varying (and usually low) resolution which covered only part of the FHILs observable in the visual spectral range. Therefore, we reobserved the objects with intermediate spectral resolution using echellette (i.e. low-order echelle) spectrograms covering the complete spectral range accessible from the ground with present CCD detectors. The observed AGN are listed in Table 1. The Seyfert types listed in this table are taken from the Veron catalog (1991). The other data in Table 1 have been derived from our spectra, as described in detail in Sections 2 and 3 of this paper.

2. Observations and data reduction

The observations were carried out during three observing runs in January, July, and November 1992 at the 2.2 m Telescope of the Calar Alto Observatory (DSAZ) near Almeria, Spain. In all cases the echellette mode of the Boller& Chivens Cassegrain spectrograph was used with a uniform slit width of 1.5 arcseconds, resulting in a (measured FWHM) spectral resolution of about R = $\lambda/\Delta\lambda$ = c/Δv = 2000. To minimize flux errors the slit was oriented parallel to the atmospheric dispersion direction. For most exposures the detector was a UV-coated 720×1152 pixel GEC CCD. During the November run a more efficient blue-sensitive $(1k)^2$ Tektronics CCD was used. With both detectors 15 spectral orders covering the wavelength range 3200 - 11 000 Å were recorded. The total exposure times per object varied between 1.2 and 7.5 hours, resulting in continuum S/N values ranging from 10 to 65 with an average of 25.

Most AGN were observed during one of the three runs only. However, for three objects the observations were repeated to search for time variations of the FHILs. But no variations of any of the FHILs could be detected.

For flux calibration during each observing night at least two spectrophotometric standard stars were observed. For $\lambda > 3800$ Å the resulting flux values are expected to be correct within about 30 % . At shorter wavelength our flux errors increase, probably as a result of differential and varying atmospheric dispersion effects. The wavelength calibration was carried out using a ThAr lamp. A spectrum of the central region of M31 obtained with the same equipment was used as a reference spectrum for the unresolved starlight contribution to the AGN spectra.

The echellette frames were reduced using routines based on standard MIDAS and IRAF software. Since the region emitting the intermediate width features is spatially unresolved and normally centered on the continuum peak, the spectra were extracted from pixels centered on the maximum of the continuum emission. Adjacent pixels were used to derive and subtract the sky contributions. Telluric absorption features were eliminated using the (intrinsically smooth) spectra of flux standards.

A comparison of the spectra in windows between the AGN emission lines with the M31 spectrum showed the presence of a significant contribution of unresolved star light to the spectra of Mrk 573 and NGC 1320. The spectra of these two objects were, therefore, corrected by subtracting the correspondingly scaled M 31 spectrum to obtain an underlying continuum free of the stellar contributions.

In all 17 spectra we searched for the presence of emission lines of H, He I, He II, [N I], [N II], O I, O III, [O I], [O II], [O III], [Ne III], [Ne V], [S II], [S III], [Ar IV], [Ar V], [Ca II], [Ca V], [Fe III], [Fe V], [Fe VI], [Fe VII], [Fe X], [Fe XI], and [Fe XIV]. For those lines which could be identified the line flux was measured. For the unblended lines the resulting flux values (normalized to Hβ) are listed in Tables A1 to A17 in the Appendix. The Hβ fluxes are given in Table A18. The fluxes for the [Fe X] 6375 Å line given in Table 1 were corrected for blending with [O I] 6364 Å by subtracting the [O I] profile derived from the [O I] 6300 Å line, assuming for the [O I] lines the theoretically predicted flux ratio of 1/3. The Hα and [N II] flux values were derived by deconvolving the corresponding blend into best fitting components. While this should have produced rather reliable results for the (always strongly dominating) Hα flux, the values derived for the red [N II] lines are less certain and should be used with appropriate caution. In those spectra with strong Fe II emission we also identified the more prominent Fe II lines. But no flux measurements of the (in most cases blended) Fe II lines were carried out.

All line flux data were corrected for interstellar reddening using the E(B-V) values listed in Table 1. The reddening values were derived applying the method of Allen (1979) to the [S II] 4068 Å, 4076 Å, [S II] 6717 Å, 6731 Å, [O II] 3726 Å, 3729 Å, and [O II] 7319 Å, and 7331 Å line pairs. The wavelength dependence of the extinction law was taken from Savage and Mathis (1979). An error analysis for the E(B-V) data in Table 1 indicates mean errors between 0.03 and 0.04 mag.

An independent reddening derivation from a comparison of the observed Balmer decrements and the (Menzel-Baker) Case B model prediction (Hα/Hβ = 2.87 for T = 10^4 K) results in slightly larger reddening values. However, according to Malkan (1983) Balmer decrements in AGN may deviate significantly from the Case B prediction. Hence, we regard the values derived from the forbidden lines as more reliable. Interestingly, the average Balmer decrement of our corrected spectra (Hα/Hβ = 3.08) is very close to the mean value found by Malkan for his sample of AGN. And it is also much closer to the theoretical value than the average decrement of the uncorrected spectra (Hα/Hβ = 3.93).

To obtain redshifts and approximate systemic velocities we calculated for each AGN the average of the observed shifts of the three emission lines [O III] 4959 Å, [O III] 5007 Å, and [O I] 6300 Å. The resulting mean redshifts are listed in the third column of Table 1. In those cases where redshifts derived from H I measurements are listed in the literature our new optical redshifts are in very good agreement with the radio data.

The redshift values of Table 1 were used to transform all spectra to the rest wavelength system. In these redshift corrected spectra we measured for all unblended lines velocity shifts of the line peaks as well as the FWHM line widths. (The [Fe X] 6375 line was again included after removal of the [O I] contribution). The resulting line profile data are also included in Tables A1 - A17. For the high-ionization lines additionally line asymmetry parameters (as defined by Heckman et al. 1981) were derived.

3. Results

3.1. Basic properties of the FHILs

In addition to the normal NLR lines and (in the case of the Seyfert 1s the BLR lines) in all observed AGN spectra the strongest lines of [Ne V] and [Fe VIII] were clearly present. Moreover, statistically significant emission of ions with even higher ionization potentials ([Fe X], [Fe XI], and in some cases [Fe XIV]) was detected in all 15 Seyfert nuclei of our sample, but not in the two radio galaxies. In all our program galaxies the FHIL emission was restriced to the unresolved core and significant extended FHIL emisssion could not be detected in our spectra.

As illustrated by the tables in the Appendix, in all spectra [Ne V] 3426 Å was by far the strongest FHIL feature. In some of our spectra [Ne V] 3426 Å is among the strongest forbidden line in the observed spectral range with a line flux comparable to that of the [O III] 5007 Å line. [Ne V] 3346 Å was less conspicuous, but usually also detected.

The Fe^{6+} lines identified by Osterbrock (1981) in Mrk 699 (= III Zw 77) were generally also visible in our spectrograms, with [Fe VII] 3760 Å and [Fe VII] 6087 Å being the strongest features. Part of our spectra also show a feature in the red wing of the Hα line which coincides in wavelength with [Fe VII] 6601.46 Å.

Examples of the observed FHILs are reproduced in Figures 1 to 3. In these figures the spectrograms are ordered according to increasing absolute line widths of the FHILs. Some of the FHILs are indicated in the top (Mrk 704) spectrum. Moreover, in the spectrum of Akn 564 (which is characterized by moderate FHILs but strong Fe II emission) we indicated the more prominent Fe II lines.

As illustrated in Fig. 1 in the AGN spectra with strong FHILs lines of [Fe VI], [Fe VII], [Fe XIV], and [Ca V] form a broad blend in the spectral range 5100 to 5400 Å. However, this region also contains strong Fe II emission lines, which also form a broad blend and which on low-resolution spectrograms often cannot be distinguished from the FHIL blend. Figure 1 shows that (with the exception of the Fe II (49) 5276.0 Å - [Fe VII] 5277.8 Å pair) at our spectral resolution the FHILs and the Fe II lines can be separated if the intrinsic line widths are not too high. From the measurements of the individual lines it is clear that in the case of Mrk 704 and Mrk 359 the broad blend is dominated by the FHILs, while in the case of Akn 564 Fe II forms the main contribution. If the lines are intrinsically broader (as in the case of the Mrk 1239 and Mrk 9) the individual contributions to the blend cannot be separated. However, a comparison of the unresolved blends with the Mrk 704 and Akn 564 spectra, shows unambiguously that in the case of Mrk 1239 the blend results essentially from unresolved Fe II lines, while in the Mrk 9 spectrum no significant Fe II contribution to the FHIL blend is present. (The weakness of the Fe II lines in Mrk 9 is confirmed by a comparison with the Mrk 1239 spectrum in Fig. 2).

In those spectra where the FHIL lines dominate, the [Fe XIV] 5303 Å + [Ca V] blend is usually a prominent feature (cf.

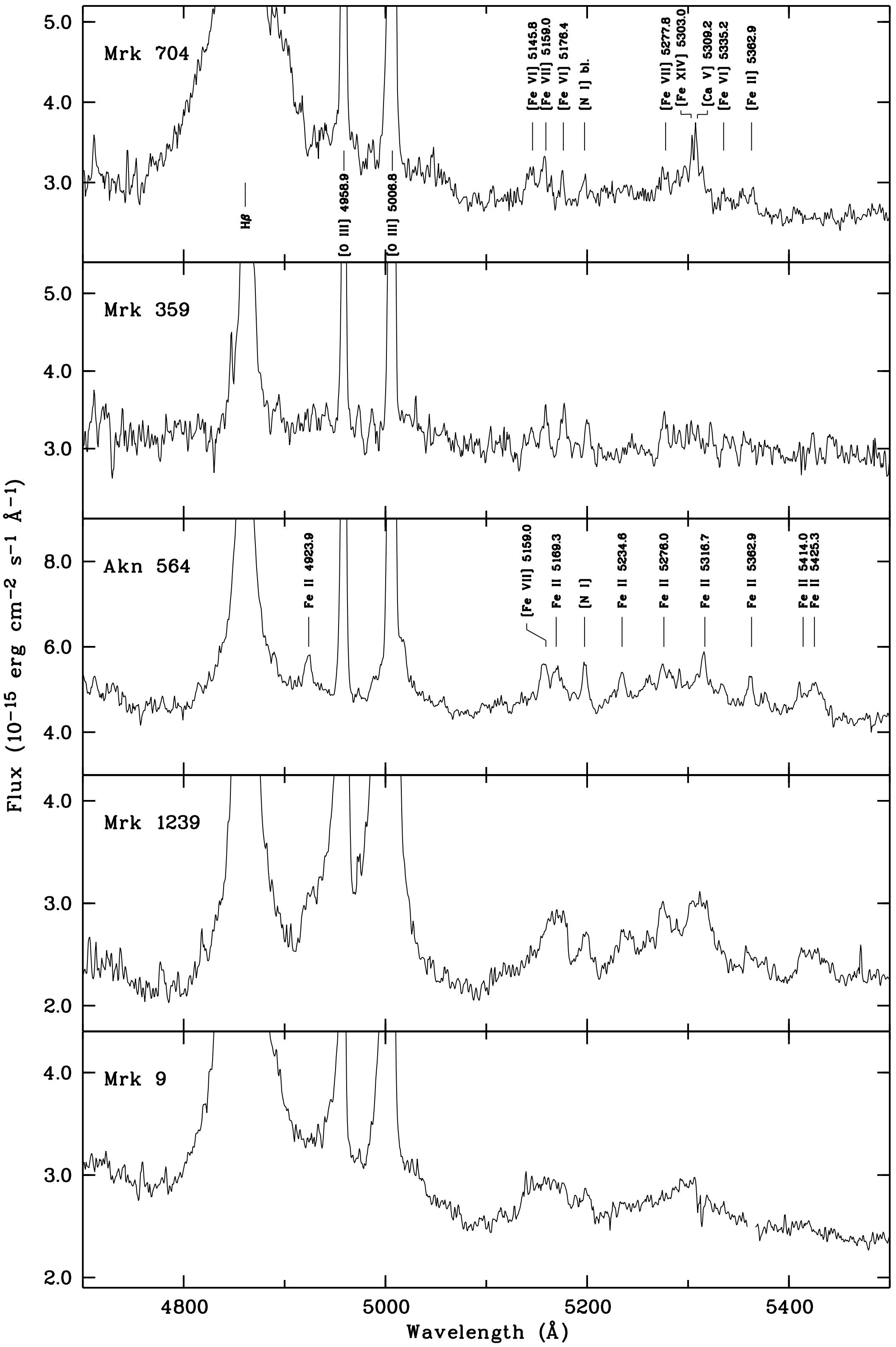

Fig. 1. Examples of forbidden high-ionization lines in the blue spectral range

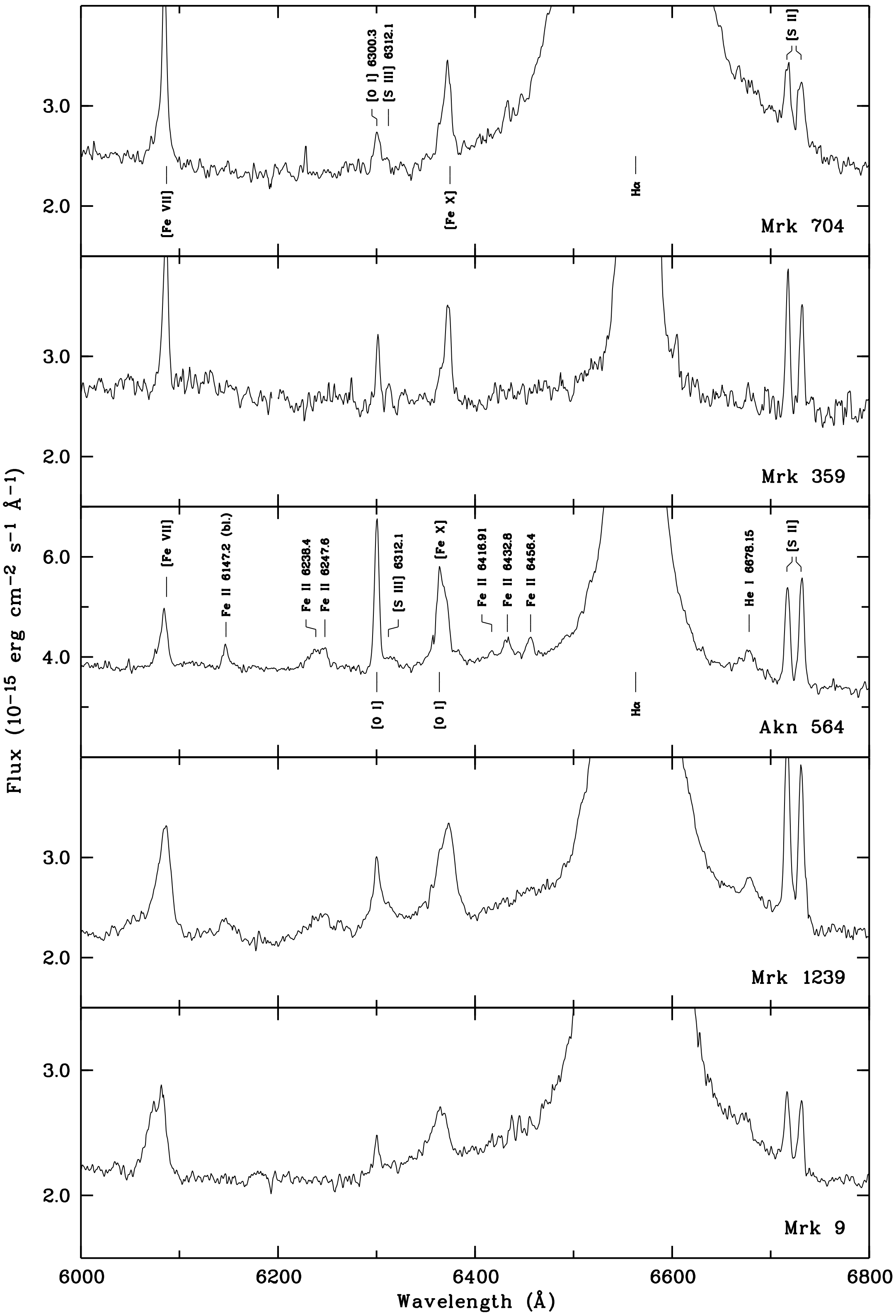

Fig. 2. Examples of forbidden high-ionization lines in the red spectral range

e.g. Mrk 704). At our resolution and S/N it is not possible to deconvolve this blend. However, if the FHILs are sufficiently narrow, then based on the the measured wavelength and profile it is possible to determine whether [Fe XIV] must be present in addition to [Ca V]. This has been found to be the situation for Mrk 699 (Osterbrock 1981) and NGC 3783 (Appenzeller and Östreicher 1988). At least our spectra of Mrk 359, Mrk 704, NGC 4151, and Mrk 699 also require the presence of a significant [Fe XIV] contribution ($>$ 25 % of the [Ca V] flux) to explain the observed blend.

Some basic properties of typical FHILs in our spectrograms are summarized in Columns 5 to 12 of Table 1. In Columns 5 to 10 we list the observed line flux and (FWHM) line width of the [Fe VII] 6087 Å, [Fe X] 6375 Å, and [Fe XI] 7892 Å lines, normalized to the corresponding values of the [O III] 5007 Å line. In Columns 11 and 12 we present the [Fe VII] 6087 Å and [Fe XI] 7892 Å line widths divided by the FWHM width of the Hα line observed in the same spectra. The mean errors of the normalized flux and line widths are in most cases less than 10 % of the values given. Exceptions are the normalized flux values $<$ 0.010 (where the errors are of the order 0.001), the flux values measured in the spectrum of Mrk 871 (which had the lowest continuum S/N of only $\approx$ 10), and the [Fe X] 6375 Å flux of Mrk 486 (see below), which are uncertain by about 20 % .

A dash in Table 1 indicates that the line in question could not be detected in the spectrum. If a question mark is given, a statistically significant feature was present, but could not be evaluated reliably, either because of poor S/N (Mrk 871), or because the atmospheric features could not be properly corrected , e.g. the [Fe XI] line of NGC 1320, which is affected by telluric H_2O absorption. Also if the lines are exceptionally broad (denoted as "br." in Table 1) the flux values are uncertain. Such exceptionally broad FHILs were observed in the spectra of Mrk 975 and Mrk 486 where FWHM widths of more than 2000 km/s are indicated for the [Fe X] and [Fe XI] lines. Such broad profiles pose a particular problem for measuring the [Fe X] 6375 Å line, since in Seyfert 1 galaxies this line coincides with the extended blue wing of the broad Hα component. Moreover, at such large line widths the wings of [Fe X] merge with [O I] 6300 Å, making a profile determination and reliable subtraction of the [O I] 6364 Å contribution to the 6375 Å blend impossible.

According to Table 1, in our AGN sample the [Fe VII] 6087 Å line flux is on average about 8 % of the [O III] 5007 Å flux, although this ratio varies greatly between different objects. The higher ionization Fe lines are on average weaker, although the change of the line flux with the ionization potential is again very different for the individual objects. In one case (Akn 564) the flux is *increasing* with ionization potential. Since Akn 564 shows strong Fe II emission, we investigated the possibility that this increase could be due to Fe II, Si II, and Ti II contamination of the [Fe X] and [Fe XI] lines. However, whilst blending with these species is known to occur, based on the known ratios with other members of the same multiplets we can be sure that their contribution to our measured fluxes of [Fe X] and [Fe XI] is small.

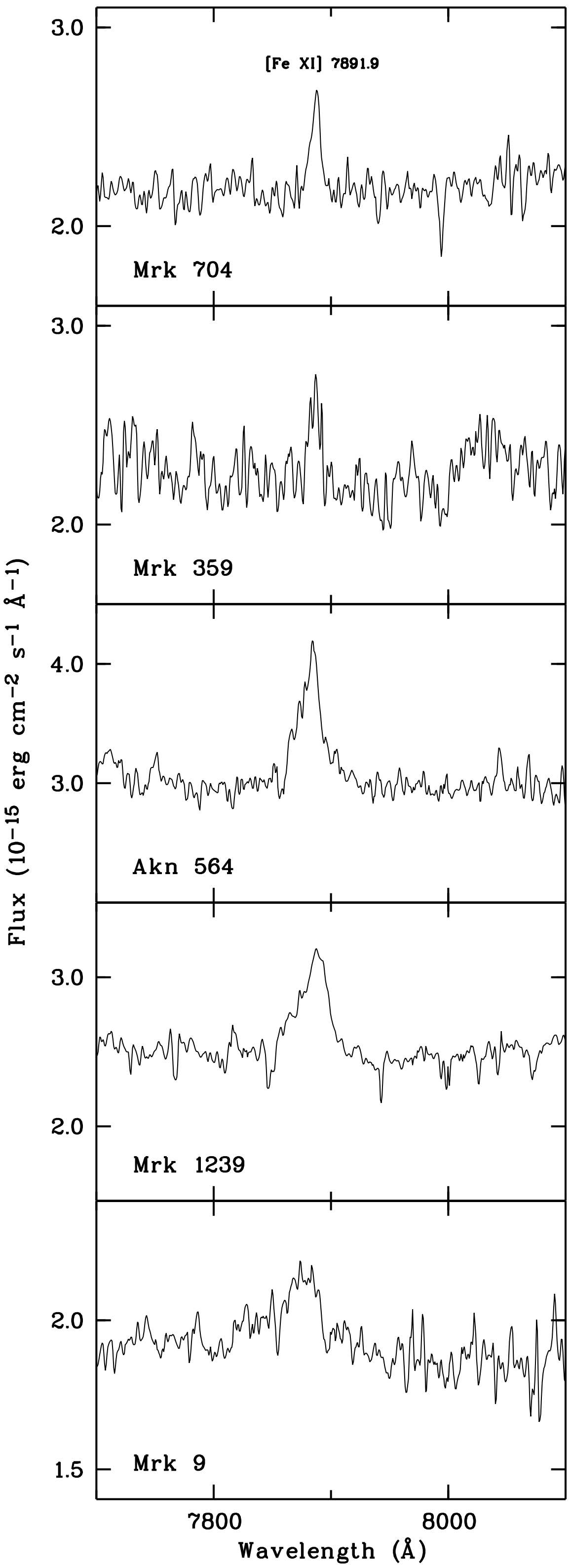

Fig. 3. The [Fe XI] 7891.9 Å line for 5 of the observed AGN

Table 1 confirms that the FHILs are in most cases significantly broader than the lower ionization forbidden lines (as qualitatively illustrated by Figs. 1 and 2), and that the line widths tend to increase with ionization potential. (This effect is larger than indicated by the last line of Table 1, since, as noted above, those objects with particularly broad lines could not be included in the averages for the [Fe X] and [FeXI] lines). In 6 of our 17 program AGN the FWHM of the FHILs are larger than or of the same order as the FWHM of the permitted Hα lines. The S/N of our spectra does not allow a more detailed profile comparison and a derivation of FW0I values for the FHILs. However, for at least one of our objects classified as a Seyfert 1 (Mrk 1239) the FW at 20 % intensity of the [Fe XI] line appears similar to the corresponding value of Hα. Hence, in some cases the wings of the FHIL profiles may be comparable or broader than the BLR profiles. But (as indicated by the last line of Table 1)in our sample the *average* widths of the FHILs are intermediate between those of the BLR and NLR.

3.2. Correlations

As indicated in Table 1, our data confirm the correlation between the line widths and the ionization potential (IP) of the FHILs. However, a formal correlation analysis resulted in a statistically significant correlation of these parameters for 1/3 of our spectra only. A more detailed analysis showed that this relatively low percentage was caused at least in part by the relatively large errors of the FWHM derivations of the weaker lines in our spectra. Because of these observational errors we could not detect the FWHM-IP correlation in the spectrum of Akn 120, the existence of which is well established from higher quality data (cf. e.g. Appenzeller and Östreicher 1988).

A larger percentage (2/3 of the investigated objects) showed a statistically significant correlation between the IP and the radial velocity displacement Δv of the lines relative to the systemic velocity. In all these cases the lines become progressively blueshifted with increasing IP. Among our sample this effect is particularly conspicuous in the spectra of Mrk 1239 and Akn 564 (Fig. 4). All those AGN in our sample where large FHIL blueshifts were observed (Mrk 975, Mrk 9, Mrk 1239, Akn 564) the FHIL profiles contained pronounced blue wings, which increase with ionization potential. As illustrated by Figure 4, at [Fe XI] these wings generally extend $> 10^3$ kms^{-1} to the blue.

A (weak) correlation was also detected between the profile parameters and the critical density of the forbidden lines. However, this may simply reflect the correlations with the ionization potential and the fact that the FHILs have, on average, higher critical densities than the lower ionization lines.

Since the FWHM and the velocity shift Δv are both correlated with the IP, there exists also a correlation between Δv and the FWHM of the FHILs of different ionization potential. However, unexpectedly, a correlation was also found between Δv and the FWHM of lines of *the same* IP. This is illustrated in Fig. 5, where we plotted the blueshift -Δv of the [Fe X] and [Fe XI] lines (which differ only little in ionization potential) as a function of the FWHM of the corresponding lines. (In addition to the data from the tables in the Appendix we also included in this diagram the corresponding values for the [Fe X] lines of NGC 3783 and Tol 0109-383 taken from Appenzeller and Östreicher 1988 and Penston et al. 1984, respectively).

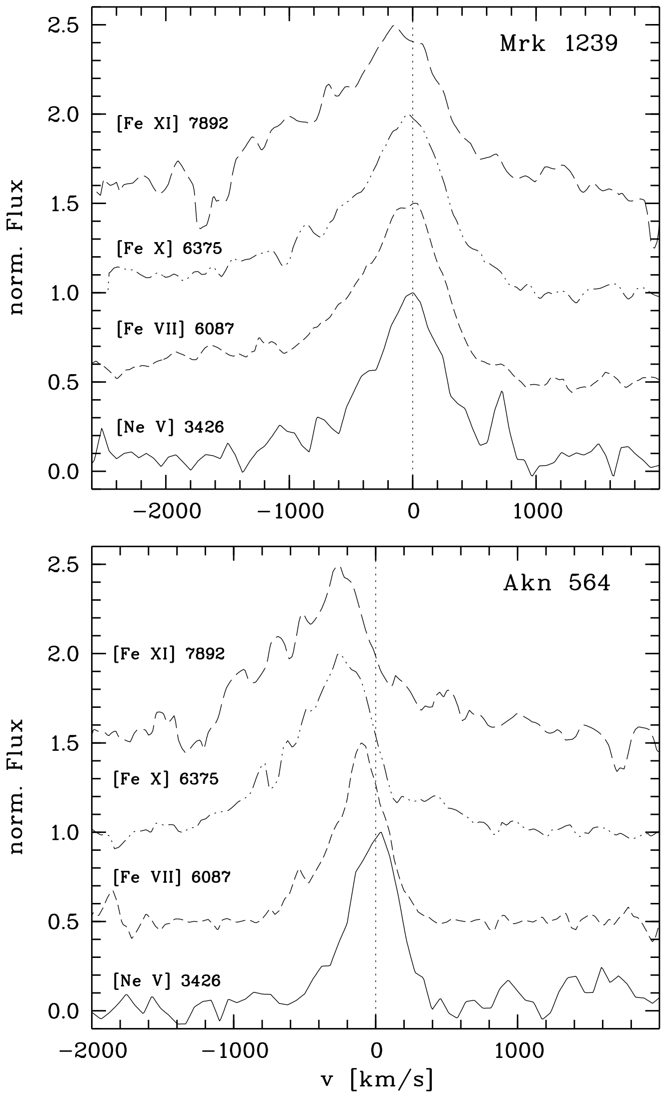

Fig. 4. Examples of the observed profiles of different forbidden high-ionization lines

As demonstrated in Fig. 5, there is a tendency of the broader FHILs to be more blueshifted, while the narrow FHILs show, on average, no or little blueshift. This correlation could be explained by the superposition of a narrow, unshifted and a broad, blueshifted component of these lines. Alternatively, there could be a common physical origin of the width and blueshift of the FHILs.

A similar, but less pronounced correlation is also observed for the [Fe VII] lines. But no such correlation could be detected for the lower ionization lines, such as [O III].

Since 6 of the 12 Seyfert 1 nuclei in our sample showed strong Fe II emission (Figs. 1 and 2) we also compared the Fe II emission strength with the observed FHIL parameters. However, no correlation or trend between the Fe II emission strength and the strength, width or deplacement of the FHILs could be detected in our sample.

3.3. Physical state of the FHIL plasma

Using the flux ratios of the line pairs [Fe VII] 3759 Å, [Fe VII] 6087 Å, and [Fe VII] 5159 Å, [Fe VII] 6087 Å and the method and numerical data of Keenan and Norrington (1987) we estimated the temperature and density of the [Fe VII] emitting gas. (In those cases where the blue [Fe VII] lines are too weak to be measured, upper limits of the temperature and electron density were derived). For our sample this procedure resulted in densities $\leq 10^7 cm^{-3}$ and temperatures of 3 - 12×10^4 K. In all AGN of our sample the temperatures and densities derived from the [Fe VII] lines are higher than the NLR values determined from [O III] and [S II] line ratios in the same spectra. As mean value of the individual derivations we obtain for the [Fe VII] regions of our AGN a temperature of 7×10^4 K and log(density)≈ 6.2. These results are similar to those estimated for the FHILs in Tol 0109-383 by Fosbury and Sansom (1983) and for NGC 3783 by Ward and Morris (1984).

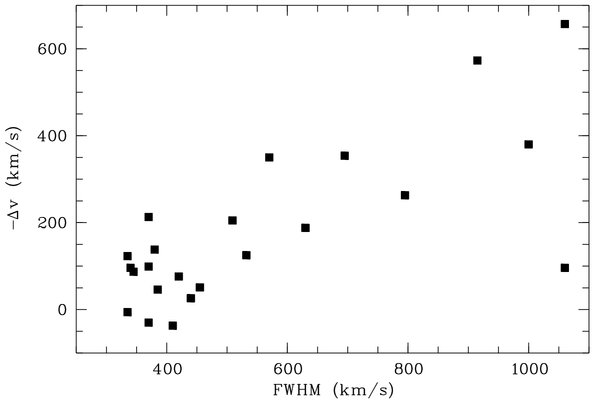

Fig. 5. Relation between the observed blueshift (-Δv) and the observed (FWHM) line width of the [Fe X] and [Fe XI] lines

In view of various error sources and since volumes with different physical conditions may contribute to the line emission, the derived numerical values of the temperature and density of the Fe^{6+} region cannot be accurate. Nevertheless, it seems clear from these estimates that the [Fe VII] lines form in a plasma which is significantly hotter than the NLR and BLR gas and which has a density intermediate between those of the BLR and the NRL.

Since for each of the ions Fe^{9+} and Fe^{10+} only one line could be detected, the physical conditions of the plasma producing these lines cannot be determined directly. However, from the smooth variation of the line profile properties with ionization potential it appears likely that the plasma containing these ions has an even higher temperature. Hence, we conclude that the plasma emitting the [Fe VII], [Fe X], [Fe XI], and [Fe XIV] lines must have an electron temperature of the order 10^5 K. In this temperature range thermal equilibrium is difficult to achieve (cf. e.g. Reynolds and Fabian 1995). The presence and observed properties of these lines, therefore, provide critical constraints for the models of the line emission regions of AGN.

The electron temperatures derived for the [Fe VII] plasma are too low to produce the observed high ionization stages of iron by electron collision. Hence an external ionization process seems to be required. For the lower ionization lines of AGN it is generally assumed that the radiation field of the central source is responsible for the ionization of the plasma. As shown by Osterbrock (1969, 1981) photoionization can also produce the high ionization stages discussed here. Simple photoionization models for FHILs have been computed by Korista and Ferland (1989) and Spinoglio and Malkan (1992). According to density values estimated above, the more compact and higher density model of Spinoglio and Malkan appears somewhat more realistic for our data than the extended low density model of Korista and Ferland, although the visual FHIL line ratios predicted by the two models are similar.

A comparison of the FHIL flux ratios derived from our data in Tables A1 - A17 with the model prediction by Korista and Ferland and by Spinoglio and Malkan shows that our (logarithmic) average flux ratios [Fe VII] 6068 Å/[Fe X] 6375 Å= 1.55, [Fe XI] 7892 Å/[Fe X] 6375 Å= .69, and [Fe VII] 6068 Å/[Fe XI] 7892 Å= 2.04 and most of the data for the individual AGN are (within the expected uncertainties) consistent with the model predictions. An exception, may be the well determined line ratios of Akn 564 where our data result in a flux ratio [Fe XI] 7892 Å/[Fe X] 6375 Å= 1.17 ± 0.10 (while the models predict values $<$0.7). Although the ratio between the [Fe VII] flux and the emission from the higher ionization stages depends critically on the (unknown) EUV flux of the continuum source (cf. Spinoglio and Malkan 1992) the [Fe XI] 7892 Å/[Fe X] 6375 Å flux ratio is less model dependent since the ratio of the abundance of Fe^{9+} and Fe^{10+} is approximately constant for a relatively large parameter range of the photoionization models. The observed high [Fe XI] flux and the variation of the [Fe XI]/[Fe X] ratio may, therefore, indicate that an additional ionization mechanism (such as shock ionization) is present in (at least) Akn 564. Models which combine photoionization and shock ionization have been proposed by Viegas-Aldrovani and Contini (1989) and by Dopita and Sutherland (1995). However, since emission from Fe ions above [Fe VII] was not included in these calculations a direct comparison with the shock ionization models is not possible at present.

3.4. Comparison with X-ray data

As described above, the observational data indicate for the FHIL emitting plasma a temperature of the order 10^5 K and densities of the order 10^6 cm^{-3}. The presence in AGN of partially ionized gas with similar properties has also been proposed independently to explain the observed X-ray continuum of the Seyfert galaxies (see, e.g., Nandra and Pounds 1992, Fabian et al. 1994, Reynolds and Fabian 1995, and the literature cited therein). In the context of models explaining the x-ray spectra the partially ionized gas producing the observed O VII and O VIII absorption edges is usually referred to as "warm absorbers". This gas is assumed to be located near the BLR or between the BLR and the NLR of the AGN. The time variability of part of the x-ray absorption indicates a stratification of the partially ionized gas along the line of sight (Otani et al. 1996, Kriss et al. 1996a, 1996b). While the inner (O VIII) zone of the warm absorbers is probably too hot to produce the FHILs observed in the visual spectra, the conditions in the outer (O VII) zone should be rather similar to those derived from the FHIL emission. Therefore, it seems attractive to assume that the FHILs form (at least in part) in the same plasma which produces the x-ray absorption edges.

If the warm absorbers and the FHIL emitting gas are related, we may expect a correlation between the x-ray absorption and the FHIL strength. Unfortunately detailed information on the warm absorbers exist for a relatively small number of AGN only. On the other hand, ROSAT PSPC data are now available for many AGN and warm absorbers can be recognized by a large photon spectral index Γ (as defined, e.g., in Walter and Fink 1993). Therefore, we plotted in Fig. 6 the ROSAT photon index Γ as a function of the equivalent width of the [Fe X] 6375 Å line for those objects in our AGN sample which are also listed in the catalog of Walter and Fink (1993). However, since Walter and Fink give Γ values for only 7 of the 17 AGN in Table 1, we added to Fig. 6 [Fe X] data taken from Penston et al. (1984; Mrk 79, Mrk 509, NGC 5548, NGC 7469, ESO 141-655), Appenzeller and Östreicher (1988; NGC 3783, IC 4329A), Filippenko and Halpern (1984; NGC 7213) and Winkler (1992, Fairall 9) and Appenzeller and Wagner (1991, PG1211+143).

Figure 6 shows that in the sample represented in this plot all AGN with strong [Fe X] emission show $\Gamma \geq 2.5$. Since 2.5 is the median value of Γ for all AGN listed by Walter and Fink, Fig. 6 seems to show that strong FHIL emission occurs only or predominantly in AGN with a soft excess, which, at least in part, are also the sources with strong warm absorbers.

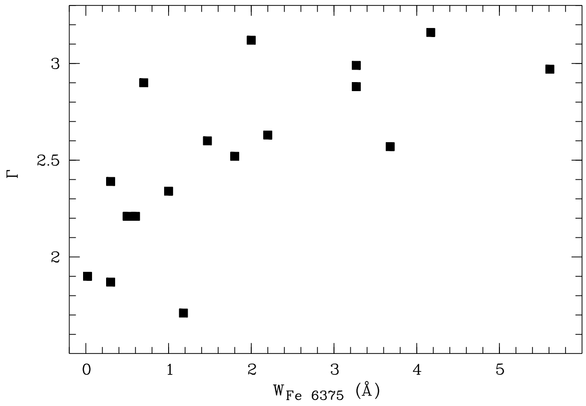

Fig. 6. Relation between the X-ray spectral index Γ and the equivalent width of the [Fe X] 6375 Å emission

3.5. The geometry of the emission region

According to the results described above, at least part of the observed FHIL emission originates from a relatively hot and moderately dense gas which shows a velocity dispersion comparable to (but on average smaller than) that of the BLR gas. The observed line widths and densities seem to indicate that these lines form closer to the central source than the NLR, possibly in the outer region of the partially ionized gas seen as "warm absorber" in the x-ray spectra. Since broad FHILs are also found in Seyfert 2s, the emission must occur outside the BLR (if the standard unified model for Seyfert 2s is correct). Although the interpretation of line shifts is, in principle, ambiguous in the case of pure emission lines, the easiest explanation for the observed blueshift and line profiles appears to be that the lines are produced in outflowing matter, where the receding part of the outflow is (partially) obscured by the dusty torus which also (again according to the standard unified model) hides the BLR of Seyfert 2s. The dependence of the observed blueshift on the ionization potential and the observed correlation between line shift and line width could in this scenario be explained by a superposition of an narrow, unshifted contribution with lower ionization (produced in or near the NLR) and the highly ionized and shifted wind contribution. As pointed out by Reynolds and Fabian (1995) and others a partially ionized outflow can be radiatively accelerated by the central source of a typical Seyfert nucleus. An important feature of such a wind model is that the temperature dependent dynamical interaction between the radiation field and the flow can produce the otherwise rather unexpected temperature range of the observed material. With the observed velocities and the densities estimated above, the mass flow in the wind is a small fraction of the accretion flow needed to power the AGN. Hence, matter evaporating from the outer regions of the accretion disk or the BLR due to the intense radiation field would be sufficient to supply the material needed to feed the wind, which is expected to expand along the radiation cones from the core.

If the radiatively accelerated wind model for the FHIL gas is correct, thermal and dynamical instabilities will be present in the flow. This will result in a breakup of the flow into clouds and in an inhomogeneous structure of the FHIL emitting region, which has to be taken into account when comparing the observations with the homogeneous models for the FHIL emission in the literature. Such instabilities could well explain the rapid variations of the O VIII zone observed at X-ray wavelengths (Otani et al. 1996), although rapid variations of the visual FHILs (produced in a larger volume) are not to be expected from such a mechanism.

The instabilities will also result in velocity differences and shocks in the flow. Hence shock ionization should definitely be present if the wind model is correct. Addition shocks may form where the wind interacts with the NLR clouds and other circumnuclear matter. These shocks may produce additional (relatively narrow and unshifted) FHIL emission from the NLR. Unfortunately, the combination of these effects will make a physically complete modelling of such a wind and the resulting line emission a complex and demanding task.

4. Conclusions

Our new spectra of a sample of AGN with strong FHILs show that the widths of these lines are correlated with the observed blueshift. While narrow FHILs show no or little blueshift, the broad FHILs show on average significant blueshifts and pronounced blue wings extending $> 10^3$ kms^{-1} towards shorter wavelengths. This blueshift can be explained assuming that the broad FHILs are produced in a radiation driven hot wind with a corresponding expansion velocity originating from the AGN's core and expanding along the radiation cones. The [Fe VII] line ratios indicate an electron temperature of the FHIL emitting matter of the order 10^5 K and densities intermediate between those of the BLR and the NLR. The observed line strengths appear compatible with predictions from simple photoionization models, although the high flux of the [Fe XI] line in Akn 465 may pose difficulties for the assumption of pure radiative ionization.

The strength of the FHIL emission was found to be correlated with the soft excess observed in the X-ray spectra of the AGN. This may indicate that the FHIL emitting wind is related to the "warm absorbers" proposed to explain the O VII and O VIII absorption edges in the X-ray spectra. On the other hand, on the basis of the present data it cannot be ruled out that the observed correlation simply reflects a dependence of the FHIL strength on the intrinsic X-ray spectrum. In order to confirm the connection between the "warm absorbers" and the FHILs higher resolution X-ray spectra of galaxies with strong FHILs would be of great value.

Because of the temperature dependence of the opacity thermal and dynamical instabilities are expected to occur in the radiation driven wind, resulting in an inhomogeneous structure of the wind and local variations of the temperature and density. This may explain the unexpected temperature and density range of the FHIL producing plasma.

A detailed test of the model outlined above will require a systematic investigation of FHILs covering a range of ionization potentials and critical densities with good spectral resolution and high S/N of selected AGN. Unfortunately, the relative weakness of the FHILs in the spectral ranges observable from the ground make such observations time consuming. Significantly stronger FHILs are present in the mid and far-IR spectral range. Some of these lines are detectable and have been observed from the ground (see e.g. Giannuzzo et al. 1995, Marconi et al. 1996). The full range of the IR FHILs will be accessible with ISO and future FIR space missions. Similarly X-ray missions with high spectral resolution and good sensitivity could be instrumental in producing more detailed information of the FHIL winds. Obviously, a combination of these techniques would offer the best promise for progress on this topic.

Acknowledgements. This work has been supported by the Deutsche Forschungsgemeinschaft (SFB 328).

References

Allen, D.A., 1979, MNRAS 186, 1P
Appenzeller, I., Östreicher, R., 1988, AJ 95, 45
Appenzeller, I., Wagner, S., 1991, A&A 250, 57
Atwood, B., Baldwin, J.A., Carswell, R.F., 1982, ApJ 257, 559
De Robertis, M. M., Osterbrock, D. E., 1984, ApJ 286, 171
De Robertis, M. M., Osterbrock, D. E., 1986, ApJ 301, 727
Dopita, M. A., Sutherland, R.S., 1995, ApJ 455, 468
Fabian, A. C., Kunienda, H., Inoue, S., et al. 1994, Publ. Astr. Soc. Japan 46, L59
Filippenko, A. V., Halpern, J. P., 1984, ApJ 285, 458
Fosbury, R. A. E., Sansom, A. E., 1983, MNRAS 204, 1231
Giannuzzo, E., Rieke, G. H., Rieke, M. J., 1995, ApJ 446, L5
Grandi, S. A., 1978, ApJ 221, 501
Heckman, T.M., Miley, G.K., van Breugel, W. J. M., Butcher, H. R., 1981, ApJ 247, 403
Keenan, F. P., Norrington, P.H., 1987, A&A 181, 370
Korista, K. T., Ferland, G. J., 1989, ApJ 343, 678
Kriss, G.A., Espey, B. R., Krolik, J. H., et al. 1996, ApJ 467, 622
Kriss, G.A., Krolik, J. H., Otani, B. R., et al. 1996, ApJ 467, 629
Malkan, M. A., 1983, ApJ 264, L1
Marconi, A., van der Werf, P.P., Moorwood, A.F.M., Oliva, E., 1996, A&A 315, 335
Nandra, K., Pounds, K.A., 1992, Nature 359, 215
Osterbrock, D.E., 1969, Astrophys. Letters 4, 57
Osterbrock, D.E., 1981, ApJ 246, 696
Osterbrock, D.E., Pogge, R. W., 1985, ApJ 297, 166
Otani, C., Kii, T., Reynolds, C. S., et al. 1996, Publ. Astr. Soc. Japan 48, 211
Pelat, D., Alloin, D., Fosbury, R. A. E., 1981, MNRAS 195, 787
Penston, M. V., Fosbury, R. A. E., Boksenberg, A., Ward, M. J., Wilson, A. S., 1984, MNRAS 208, 347
Reynolds, C. S., Fabian, A. C., 1995, MNRAS 273, 1167
Savage, B. D., Mathis, J. S., 1979, ARA&A 17, 73
Spinoglio, L., Malkan, M. A., 1992, ApJ 399, 504
Thompson, R. I., 1996, ApJ 459, L61
van Groningen, E., de Bruyn, A. G., 1989 A&A 211, 293
Veron-Cetty, M.-V., Veron, P., 1991, A Catalog of Quasars and Active Nuclei (5th edition), ESO Scientific Report No. 10
Viegas-Aldrovani, S. M., Contini, M., 1989, A&A 216, 253
Wagner, S., 1997, in "Emission Lines in Active Galaxies: New Methods and Techniques", Proc. IAU Colloquium 159, eds. B. M. Peterson et al. (ASP Conference Series, in press)
Walter, R., Fink, H.-H., 1993, A&A 274, 105
Ward, M., Morris, S.,1984, MNRAS 207, 867
Whittle, M., 1985, , K. A., MNRAS 216, 817
Wilson, A.S., 1979 Proc. R. Soc. London Ser. A 366, 461
Wilson, A. S., Nath, B., 1990, ApJS 74, 371
Winkler, H., 1992, MNRAS 257, 677

Appendix

Tables A1 to A18: Observed flux values, velocity shifts, and line widths of emission lines in the spectra of our programme galaxies.

These tables are only available in electronic form at the CDS (Strasbourg) via anonymous ftp to cdsarc.u-strasbg.fr (130.79.128.5) or via http://cdsweb.u-strasbg.fr/Abstract.html.

This article was processed by the author using Springer-Verlag LaTeX A&A style file *L-AA* version 3.